Journal of Industrial and Engineering Chemistry 16 (2010) 193–199

Contents lists available at ScienceDirect

Journal of Industrial and Engineering Chemistry

journal homepage: www.elsevier.com/locate/jiec

Measurement of the hydroxyl radical formation from H_2O_2, NO_3^-, and Fe(III) using a continuous flow injection analysis

Bum Gun Kwon [a,*], Jung-Hwan Kwon [b]

[a] Department of Environmental Science and Engineering, Gwangju Institute of Science and Technology (GIST), 1 Oryong-dong Buk-gu, Kwangju 500-712, Republic of Korea
[b] Department of Environmental Engineering, Ajou University, Woncheon-dong, Yeongtong-gu, Suwon 443-742, Republic of Korea

ARTICLE INFO

Article history:
Received 9 April 2009
Accepted 6 October 2009

Keywords:
Quantum yield
Hydroxybenzoic acid
Advanced oxidation process
Photo-degradation

ABSTRACT

Production of hydroxyl radical (•OH) is of significant concern in engineered and natural environment. A simple in situ method was developed to measure •OH formation in UV/H_2O_2, UV/Fe(III), and UV/NO_3^- systems using trapping of •OH by benzoic acid (BA) and measuring fluorescence signals from hydroxylated products of BA. Method development included characterization of •OH trapping mechanism and measurement of quantum yields ($\Phi_{\bullet OH}$) for •OH. The distribution of OHBA isomers was in the order of *o*-OHBA > *p*-OHBA > *m*-OHBA, although it changed with the H_2O_2 concentration and light intensity. This supports that •OH attacks dominantly on the benzene rings. The quantum yields for •OH formation in the UV/H_2O_2 process were 1.02 and 0.59 at 254 and 313 nm, which were in good agreement with the literature values, confirming that the method is suitable for the measurement of •OH production from UV/H_2O_2 processes. Using the continuous flow method developed, quantum yields for •OH in UV/H_2O_2, UV/Fe(III), and UV/NO_3^- systems were measured varying the initial concentration of •OH precursors. The $\Phi_{\bullet OH}$ values increased with increasing concentrations of H_2O_2, Fe(III), and NO_3^- and approached constant values as the concentration increased. The $\Phi_{\bullet OH}$ values were 0.009 for H_2O_2 at 365 nm, showing that •OH production is not negligible at such high wavelength. The $\Phi_{\bullet OH}$ values during the photolysis of $Fe(OH)^{2+}$ (pH 3.0) and $Fe(OH)_2^+$ (pH 6.0) at 254 nm were 0.34 and 0.037, respectively. The $\Phi_{\bullet OH}$ values for NO_3^- approached a constant value of 0.045 at 254 nm at the initial concentration of 10 mM.

1. Introduction

Photochemical processes, such as ultraviolet/hydrogen peroxide (UV/H_2O_2) process, are one of the most extensively studied advanced oxidation processes (AOPs) and have become commercially available for the removal of contaminants in water and wastewater [1,2]. It has become more and more important with increasing demands on the quality of treated water and the growing necessity for an integrated water treatment system [3,4]. The hydroxyl radical (•OH) generated in the photochemical processes is a non-selective and reactive oxidant, initiating the degradation of organic pollutants [5]. These OH radicals are known to be generated by the photolysis of nitrate (NO_3^-) and iron(III) species as well as hydrogen peroxide (H_2O_2) both in the natural environment and in engineered systems [6–9].

Various instrumental methods have been used for measuring •OH, including electron spin resonance (ESR) [10], high-performance liquid chromatography [11], and fluorescence (FL) [12–14]. FL method is superior to others because of inexpensive equipments required, convenient operation, high selectivity and sensitivity, and better reproducibility [14,15]. In addition, FL measurement of the hydroxyl radicals can be achieved in a flow injection analysis (FIA) system, which enables us to obtain real-time data [16]. FL method requires fluorescence probes for detecting •OH, such as benzoic acid (BA)/benzoate [17–19], salicylic acid [17], terephthalic acid [15], and *p*-chlorobenzoic acid [20]. Among these hydroxyl radical probes, the reaction of •OH with BA has been widely examined in pulse radiolysis [12,13,17–19,21], Fenton reaction [19], and TiO_2 photocatalysis [22]. The first step of this mechanism is a very fast nucleophilic addition of the hydroxyl radical on BA [10], leading to the formation of an intermediate, cyclohexadienyl radical, which is rapidly oxidized to its hydroxylated derivatives, *o*-, *m*-, and *p*-hydroxybenzoic acid (OHBA) isomers [12,13,23]. Various distribution of *o*-, *m*-, and *p*-OHBA isomers formed by •OH was found in the literature [11,23]. Since the ratio of OHBA isomers was depended on processes and experimental conditions, it still

* Corresponding author. Present address: School of Chemical and Biological Engineering, Seoul National University, Kwangju 500-712, Republic of Korea. Tel.: +82 2 880 8941; fax: +82 2 876 8911.
E-mail address: kwonbg0@daum.net (B.G. Kwon).

1226-086X/$ – see front matter © 2010 The Korean Society of Industrial and Engineering Chemistry. Published by Elsevier B.V. All rights reserved.
doi:10.1016/j.jiec.2009.10.007

remains to be demonstrated that the yield of OHBA correlates with the yield of •OH at a specified irradiation wavelength with respect to the concentration of H_2O_2.

The quantum yield (Φ•OH) for OH radicals plays a very important role in determining the efficiency of pollutants' photo-degradation [2,6,8,24–26]. Thus, it is crucial to have a better understanding of the processes forming hydroxyl radicals by the photochemical reactions. However, these values have not been reported rigorously over the range of all relevant wavelengths for •OH precursors.

The Φ•OH during the photolysis of H_2O_2 has been known to be approximately 1 at 254 nm [9,27]. Many researchers have looked into the decomposition of organic pollutants during wastewater treatment with •OH formed by the H_2O_2 photolytic processes [1–4]. However, Φ•OH on the decomposition of H_2O_2 at ultraviolet light, *i.e.*, $\lambda > 313$ nm, are no or limited published data on the photochemical formation of •OH in the aqueous solution based on the incident light intensity, even though the photochemical reaction of H_2O_2 in an aqueous solution may occur measurably even at 365 nm [28,29]. For nitrate, on the other hand, most of the past studies have measured Φ•OH at wavelength >300 nm [6], and there is no published data on Φ•OH in the aqueous solution at 254 nm. It may be due to that most of the past •OH detection methods were not sensitive enough to trace products [11] and •OH has a very short lifetime. Similarly, most of the past studies have measured Φ•OH by the photolysis of Fe(III)-hydroxo complexes at wavelength >300 nm. In particular, Benkelberg and Warneck [7] obtained extensive Φ•OH on Fe(III)-hydroxo complexes over a wide range of wavelength (>280 nm) by monitoring the acetone produced by the reaction of 2-propanol as a probe with •OH. Then, Lee and Yoon [8] have recently re-investigated Φ•OH for the photolysis of Fe(III)-hydroxo complexes in the wavelength range 240–380 nm by a kinetic method using dimethylsulfoxide (DMSO) as a •OH probe. Under those experimental condition, the Fe(III)-hydroxo complexes were concurrently existed in the Fe^{3+} and $Fe(OH)^{2+}$ forms (≈99% of total iron concentration), and the Φ•OH for each Fe(III)-hydroxo complex was kinetically determined [8]. Thus, it is required to apportion effects of ferric species in the aqueous solution.

The main objective of this study was to investigate the Φ•OH in UV/H_2O_2, UV/Fe(III), and UV/NO_3^- systems by using a continuous FIA. The distribution of OHBA isomers formed in the UV/H_2O_2 process was examined under three selected wavelengths (254, 313 and 365 nm) during a short irradiation time (<3 min) in order to avoid secondary reactions of OHBA isomers formed. The secondary reactions of OHBA isomers were examined with the FL analytical method reported by Armstrong et al. [12]. At the same time, we measured Φ•OH by direct photolysis of H_2O_2 at 254, 313, and 365 nm, since the Φ•OH is one of the most useful quantities in the study of photochemical reactions. The quantum yields of hydroxyl radicals formed from nitrate and Fe(III) at 254 nm were also measured by varying initial concentrations of nitrate and Fe(III).

2. Materials and methods

2.1. Materials

BA (99.9%), 3% H_2O_2, *o*-OHBA (99+%), *m*-OHBA (99%), *p*-OHBA (99+%), methanol (99.8+%), 2,4-pentanedione (99+%), ammonium acetate (97+%), 37% formaldehyde, sodium nitrate, ferric sulfate, horseradish peroxidase (type VI), *p*-hydroxyphenylacetic acid, potassium permanganate, and 1,10-phenanthloline (99%) were obtained from Sigma–Aldrich (St. Louis, MO, USA) and were of reagent grade. The concentration of the H_2O_2 stock solution was determined by a $KMnO_4$ titration method prior to use. Working solution of H_2O_2 was prepared daily by diluting the stock solution with deionized water. The concentration of formaldehyde stock solution was determined by EPA Method 8315A [30]. The working standards of HCHO were prepared by serial dilution of the stock standard. Stock solutions of nitrate and ferric ions were prepared daily and stored in the dark at 4 °C. In particular, the ferric solution was prepared from deionized water at pH 3 adjusted with sulfuric acid and pH 5.8 with deionized water and sodium hydroxide. Other solution pH was adjusted to be between 5 and 8 using 0.01 M H_2SO_4 and/or 0.1 M NaOH.

2.2. Photochemical equipment and experimental procedure

Fig. 1 shows a schematic diagram of the apparatus used in this study. The photochemical reaction was taken place in a small coil-type tube quartz reactor (i.d. 2, 900 mm long; reaction

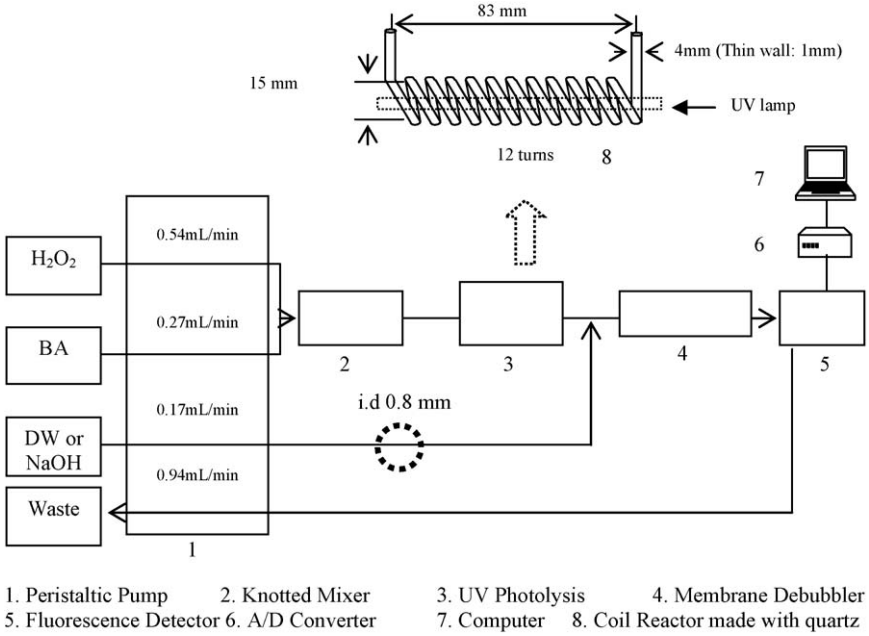

Fig. 1. The schematic diagram for UV photolysis and the continuous flow injection analysis system used in this study.

volume ≈ 3.02 cm^3). UV lamp (4-W low pressure Hg; Sankyo Denkyo, Japan) was placed in the inner center of the reactor [31] at the specified wavelengths of 254, 313, and 365 nm. The light source has relatively narrow wavelength range. For example, 365 nm source used in this study ranges 320–380 nm at peak intensity at 365 nm.

All solutions including H_2O_2 and BA were delivered using a peristaltic pump (Ismatec, type ISM 946, Vernon Hills, IL, USA) with PTFE tubing (i.d. 0.8 mm; Cole-Parmer, Vernon Hills, IL, USA) and were primed in the coil-type tube reactor before photolysis. In the reactor, H_2O_2 cleaves by absorbed light and produces hydroxyl radicals, where the formed hydroxyl radicals react with BA producing OHBA isomers [31]. In order to exclude the secondary reaction of OHBA isomers by additional hydroxyl radicals, the photochemical reaction time at 254 and 313 nm was limited to <1 min, whereas that at 365 nm was up to 3 min. Under these reaction times, the secondary reaction of OHBA isomers is thought to be negligible based on FL analytical method reported by Armstrong et al. [12]. The reactor was cooled by a cooling fan because $\Phi_{\bullet OH}$ might increase with increasing temperatures [32]. After passing the photochemical reactor, solution streams containing OHBA isomers were mixed in the 1 m knotted tubing reactor (KTR) (PTFE, i.d., 0.8 mm) [33]. Air bubbles formed during mixing were removed by incorporating a small piece (length, 3 cm) of porous hydrophobic membrane tube (Gore-Tex TA 001, Gore and Associates, Elkton, MD, USA) [34], prior to the entry to a 16 μL flow-through cell in a FL detector (Waters, 474 Model) [31]. The fluorescence signal was transferred to a data acquisition system, consisted of a signal amplifier, an analog-to-digital converter, and a personal computer.

2.3. Analysis

The conversion of BA into OHBA isomers was analyzed by FL detection. The FL intensities of *o*-OHBA and *m*-OHBA were measured at 410 nm with the excitation wavelength of 314 nm under an acidic condition (pH 4.9) buffered by acetate and under an alkaline condition (pH ≥ 11) with 0.05N of NaOH, respectively, at which the FL intensities of OHBAs were maintained at their maximum level [12,31]. The FL intensity of *p*-OHBA was determined at 330 nm with the excitation at 285 nm under the basic condition mentioned above. All analyses were carried out in duplicate or triplicate and all calibrations were performed using signal heights.

In order to investigate the photochemical $^{\bullet}OH$ formation, a formaldehyde determination method using the Hantzsch reaction was used because it uses fast and sensitive fluorometric procedure with excellent precision [35]. The specific use of 2,4-pentanedione and ammonium acetate for the determination of formaldehyde leads to 3,5-diacetyl-1,4-dihydrolutidine, which fluoresces at 510 nm with the excitation at 410 nm.

H_2O_2 concentration was measured using a horseradish peroxidase method, based on the reaction between H_2O_2 and (*p*-hydroxypheny1)acetic acid, catalyzed by horseradish peroxidase, generating a fluorescent dimer. Further details were reported by Lee et al. [36].

A UV spectrophotometer (Shimadzu, UV1601 Model, Japan) was used for measuring changes in the absorption spectra for Fe(III), hydrogen peroxide and nitrate with quartz cells having a 1 cm optical path length, as well as the molar extinction coefficients of H_2O_2, BA, and OHBA isomers.

2.4. Quantum yield and light intensity

The quantum yield for the production of hydroxyl radical ($\Phi_{\bullet}$OH) is defined as the number of molecules formed per unit volume per time divided by the quanta of light absorbed per unit volume per unit time [29]:

$$\Phi_{\bullet OH} = \frac{R_{OH}}{R_I} \tag{1}$$

where $R_{\bullet}$OH is the formation rate of $^{\bullet}OH$ (M s^{-1}) and R_I is the light intensity (einstein L^{-1} s^{-1}).

The incident light intensity was analyzed by a chemical actinometer. Ferrioxalate (6 mM) in the coil-type tube reactor was reduced when exposed to UV light [29,37] and formed ferrous ion, which forms a stable complex with 1,10-phenanthroline. The ferrous-1,10-phenanthroline complex was detected by a UV/vis spectrophotometer (730D Model; YoungLin Co., Korea) equipped with a flow-through quartz cell with 1 cm light path length at 510 nm. Reaction time for the Fe(II)-complexation was at least 5 min [38] in a 10 m KTR before being run through the UV detector. The light intensity within the system can be expressed using Lambert–Beer's law as follows:

$$\frac{d[Fe^{2+}]}{dt} = \Phi I_o[1 - \exp(-2.303 L \varepsilon_a C)] \tag{2}$$

where Φ is the quantum yield of ferrioxalate, *i.e.*, 1.24–1.25, for wavelengths of 254 and 313 nm, I_o is the incident UV light intensity, L is the length of the light path, and ε_a is the absorption coefficient of ferrioxalate (11,000 M^{-1} cm^{-1}) [29]. If $2.303\Phi\varepsilon_a L[Fe^{3+} - Ox] > 2$, Eq. (2) can be simplified to Eq. (3):

$$I_o = \frac{d[Fe^{2+}]/dt}{\Phi}. \tag{3}$$

Thus, we can determine the light intensity based on the quantum yields of Hatchard and Parker [37] and the experimental results of ferrous ion formation rate (M s^{-1}) in this study.

From Eq. (4), we can determine the length of the light path (L) as follows:

$$-\frac{d[H_2O_2]}{dt} = \Phi I_o[1 - \exp(-2.303 L \varepsilon_a [H_2O_2])] \tag{4}$$

$$L = \frac{-d[H_2O_2]/dt}{2.303\Phi I_o \varepsilon_a [H_2O_2]} \tag{4-1}$$

where Φ is the quantum yield of H_2O_2, and ε_a for H_2O_2 is 19.6 M^{-1} cm^{-1} at 254 nm (Table 1). Eq. (4) is simplified to Eq. (4-1) using the Taylor series approximation if H_2O_2 concentration is low (<20 μM). Thus, L is simply determined, if the decomposition rate of H_2O_2 in our coil reactor is measured. The light path in the coil-type tube reactor was determined to be 1.53 cm.

3. Reaction scheme

In the UV/H_2O_2 system, H_2O_2 is photo-decomposed to produce two $^{\bullet}OH$ by UV absorption (reaction (1)) (Table 1), and a series of reactions propagate and terminate as shown in reactions (5)–(11). The principal reaction mechanisms are listed below [1,14,31]:

$$H_2O_2 + h\nu \rightarrow 2^{\bullet}OH, \quad k_1 = 2.303\Phi\varepsilon_a L[H_2O_2] \tag{5}$$

$$^{\bullet}OH + H_2O_2 \rightarrow HO_2^{\bullet}/O_2^{\bullet -} + H_2O, \quad k_2 = 2.7 \times 10^7\ M^{-1}\ s^{-1} \tag{6}$$

$$HO_2^{\bullet} \leftrightarrow H^+ + O_2^{\bullet -}, \quad pK_a = 4.8 \tag{7}$$

$$HO_2^{\bullet} + HO_2^{\bullet} \rightarrow H_2O_2 + O_2, \quad k_4 = 7.61 \times 10^5\ M^{-1}\ s^{-1} \tag{8}$$

$$HO_2^{\bullet} + O_2^{\bullet -} \rightarrow HO_2^{-} + O_2, \quad k_5 = 8.86 \times 10^7\ M^{-1}\ s^{-1} \tag{9}$$

$$O_2^{\bullet -} + O_2^{\bullet -} \rightarrow O_2 + O_2^{2-}, \quad k_6 < 0.3\ M^{-1}\ s^{-1} \tag{10}$$

Table 1
The molar extinction coefficients of H_2O_2, benzoic acid, and *o*-, *m*- and *p*-hydroxybenzoic acid (OHBA).

Components	λ (nm)	Extinction coefficient ($M^{-1}\,cm^{-1}$)	References
H_2O_2	313	0.54 ± 0.09	This study
	254	19.52 ± 0.02	This study
	313	0.40	[9]
	254	19.6	[9]
Benzoic acid	313	–	This study
	254	1092 ± 103	
	230	9501 ± 219	
o-OHBA	313	1564 ± 52	This study
	254	399 ± 23	
	230	7186 ± 445	
m-OHBA	313	–	This study
	254	918 ± 28	
	230	6486 ± 222	
p-OHBA	313	–	This study
	254	2401 ± 91	
	230	10,391 ± 320	

$$^{\bullet}OH + BA \rightarrow o\text{-},m\text{-},p\text{-OHBA}, \quad k_7 = 4.3 \times 10^9\ M^{-1}\,s^{-1} \qquad (11)$$

Radical chain reactions can be terminated by the reaction between •OH and excess BA (≥0.1 mM) (reaction (11)). As shown in reactions (6) and (11), BA may compete with H_2O_2 for •OH. However, approximately 97–99% of •OH reacts with BA, whereas <3% of •OH reacts with H_2O_2, considering the reaction rates of reaction (11) to reaction (6) under the given experimental condition. Hence, reactions (6–10) can be ignored due to the termination reaction with BA and to a weak reaction between BA and $HO_2^{\bullet}/O_2^{\bullet-}$. In addition, $HO_2^{\bullet}/O_2^{\bullet-}$ produces H_2O_2 and O_2 in the aqueous solutions and spontaneous self-reactions are significantly slow compared to the rate of OHBA formation [39]. Thus, it is reasonable to assume that most of hydroxyl radicals formed under UV irradiation reacts with excess BA giving OHBA.

4. Results and discussion

4.1. Control experiments and detection limits

Preliminary and control experiments were performed to investigate the stability and detection limits of BA and OHBA isomers in an irradiated system without H_2O_2 as well as in a system containing H_2O_2 that was kept in the dark. The control test in the absence of UV showed no FL signal, showing that BA is very stable in the presence of H_2O_2. Methanol used as an alternative probe for •OH was also highly stable under dark condition in the presence of H_2O_2. Direct photolysis of methanol in deionized water instead of aqueous H_2O_2 solution showed no detectable FL signal of HCHO, whereas the direct photolysis of BA at 254 nm in deionized water showed a detectable formation of OHBAs (approximately 10 nM level) at pH ≥ 10. This OHBA formation would be derived from the UV absorbance at 254 nm because the molar extinction coefficient of BA at 254 nm was found to be 1092 $M^{-1}\,cm^{-1}$ (Table 1). However, there were no characteristic FL signals at 313 and 365 nm.

The detection limit for OHBA isomers was estimated as the signal-to-noise ratio of 2. The FL signals of a sample containing solutions of BA and methanol were used as a baseline for the FL detector in these experiments during dark control experiments. The detection limit of the standard solutions was found to be 26 nM for *o*-OHBA, 13 nM for *m*-OHBA, and 23 nM for *p*-OHBA. The detection limit of HCHO was estimated to be 5.85 nM.

4.2. Light intensity and light path length in a coil-type tube reactor

The formation of •OH during the UV/H_2O_2 process depends on the concentration of H_2O_2, the light intensity and wavelength, the concentration of the •OH scavengers, and type or shape of the reactor [29,40]. Among all these factors, both the light intensity and the light path length are the most useful and fundamental parameters. As shown in Table 2, the light intensities (I_o) were 3.27×10^{-5}, 3.13×10^{-5}, and 1.55×10^{-5} einstein $L^{-1}\,s^{-1}$ at 254, 313, and 365 nm, respectively.

4.3. Distribution of the isomeric OHBA and trapping efficiency of BA on •OH

Table 2 shows the yields of *o*-, *m*- and *p*-OHBA varying concentrations of H_2O_2 and BA at three selected wavelengths. The distribution of OHBA isomers did not depend on BA concentration between 0.1 and 10 mM. The fractions of OHBA isomers were in the order of *o*-OHBA > *p*-OHBA > *m*-OHBA. These results indicate that •OH attacks dominantly on the benzene rings [41,42], instead of decarboxylation of BA, resulting in the formation of OHBA isomers. The yields of *o*- and *p*-isomers are relatively higher than that of

Table 2
The distribution of hydroxybenzoic acid isomers under various experimental conditions and corresponding quantum yield.

Experimental conditions				*o*-OHBA (mM)	*m*-OHBA (mM)	*p*-OHBA (mM)	Quantum yield (Φ.OH)
λ (nm)	$[H_2O_2]_{Inj}$ (mM)	$[BA]_{Inj}$ (mM)	I_o (einstein/s)				
365	1	0.1	1.55×10^{-5}	0.017	0.007	0.028	0.009 ± 0.001[a]
	1	1		0.023	0.009	0.037	
	1	2.5		0.030	0.017	0.054	
	5	10		0.041	0.027	0.074	
	10	10		0.047	0.032	0.086	
313	0.5	0.1	3.13×10^{-5}	0.020	0.013	0.020	0.59 ± 0.01[a]
	1	1		0.057	0.033	0.037	
	2.5	2.5		0.106	0.071	0.095	
	5	8		0.203	0.145	0.206	
	10	10		0.231	0.135	0.215	
	15	10		0.245	0.153	0.203	
254	0.5	0.1	3.27×10^{-5}	0.056	0.051	0.055	1.03 ± 0.05[a]
	1	1		0.182	0.122	0.172	
	2.5	5		0.179	0.150	0.176	
	5	8		0.347	0.134	0.283	
	10	10		0.443	0.153	0.432	
	15	10		0.453	0.147	0.413	

[a] Average and standard deviation of five replicates.

m-isomer under almost all experimental conditions except at high H_2O_2 concentrations and the lower wavelength (254 nm). This is in good agreement with the results by Armstrong et al. [12] in their radiolysis of BA, and by Eberhardt and Yoshida [42] and Matthews and Sangster [21] in their aromatic substitution studies with nitrophenol and phenol.

Although OHBA isomers are the major reaction products during the UV/H_2O_2 process, other secondary products such as dihydroxybenzoic acid and decarboxylated compounds of benzoic acid might form as by-products [23]. Dihydroxybenzoic acid is a minor product and the decarboxylation of benzoic acid via the •OH is not significant, with an occurrence of about 7% [12,13]. Furthermore, if the reaction time is <3 min as was in this study, the secondary reaction of OHBA isomers formed has been known to be negligible [12].

The reaction mechanisms of BA and methanol with •OH have distinct characteristics [43]. Methanol was used as a well-known •OH probe in this study to examine the trapping efficiency of BA and to eliminate any possible bias of a single probe. The hydroxylation of BA is more efficient than formaldehyde formation by alpha hydrogen abstraction (see Supplementary Data, Fig. S1). Thus, the hydroxyl radical trapping efficiency of BA seems to be very high and it is reasonable to assume that the trapping of the hydroxyl radical can be enhanced by increasing the BA concentration.

4.4. Rate of •OH formation

Disappearance of H_2O_2 usually follows a first-order kinetics in a UV/H_2O_2 system and the concentration of •OH formed increases with the concentration of H_2O_2. If the concentration of BA is sufficiently high, the hydroxyl radicals formed will primarily react with BA and produce OHBA isomers. Hence, the •OH formation rate translates into the rate of OHBA formation as follows:

$$\frac{d[\mathrm{OHBA}]}{dt} = k_{\mathrm{BA}}[^{\bullet}\mathrm{OH}][\mathrm{BA}] \quad (12)$$

Therefore, as [BA] increases, OHBA formation will prevail, and the OHBA isomers will not react significantly with •OH radicals provided that concentration of BA and the flow rate in the reactor are sufficiently high.

Fig. 2 shows that the formation rate (M s^{-1}) of OHBA isomers increased with increasing initial H_2O_2 concentration between 1 and 20 mM at all wavelengths investigated (BA = 10 mM and pH 5.8). Production of •OH at near visible wavelength (365 nm) was identified although the rate is much slower than those at the lower wavelength. At 365 nm, the formation rate of OHBA increased with increasing H_2O_2 concentration and became constant at 10 mM H_2O_2, and was found to be from 4.34×10^{-9} M s^{-1} ($[H_2O_2]_o$ = 1 mM) to 1.33×10^{-7} M s^{-1} ($[H_2O_2]_o$ = 10 mM) at 365 nm, as shown in Fig. 2. The direct photolysis of aqueous BA at 365 nm instead of aqueous H_2O_2 solution showed no detectable FL signal of OHBA isomers, similar to the result of formaldehyde formation by using methanol probe. Thus, this result indicates that H_2O_2 solution is photolyzed even at 365 nm to produce OH radicals.

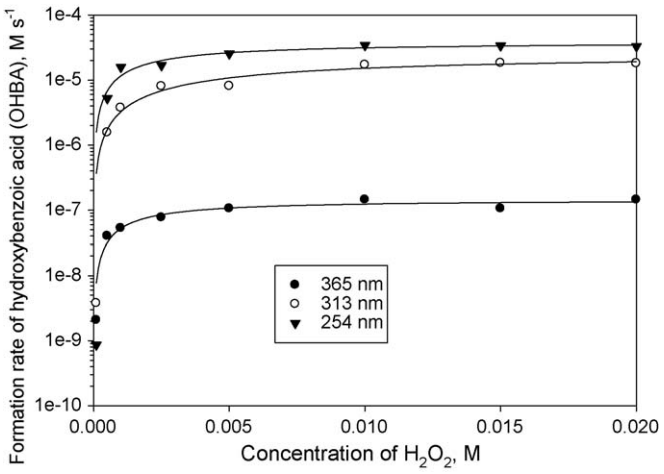

Fig. 2. Effects of H_2O_2 concentration on the rate of hydroxyl radical formation. Solid lines show trendlines.

However, the presence of other •OH scavengers may depress the formation of OHBA. The scavenging effects of •OH by chloride show the decreases of OHBA concentration (see Supplementary Data, Fig. S2). For example, the concentration of total OHBA was reduced down to 16 nM even at the chloride concentration of 5 mM. The second-order rate constant for chloride with •OH is 4.2×10^9 M^{-1} s^{-1} [10]. Since the non-selective •OH can be easily scavenged by chloride, it would be important to assess the concentration of residual chloride ions as an •OH scavenger.

4.5. Method validation and quantum yields for •OH

Quantum yields for •OH (Φ•OH) in the UV/H_2O_2 process are presented in Table 2. The analytical method using BA for •OH measurement was verified by determining a well-known Φ•OH from direct photolysis of H_2O_2 at 254 and 313 nm, respectively. The yields of the OHBA isomers increased with increasing concentrations of BA and H_2O_2. Since the formation of the OHBA isomers depends on the concentrations of both H_2O_2 (below 15 mM) and BA (approximately 10 mM) at each wavelength, Φ•OH has been greatly increased. Φ•OH obtained at 254 nm was 1.02 (Table 2), which is in good agreement with the literature values [9,27,28]. The Φ•OH value at 313 nm was determined as 0.59 (Table 2), which is again in good agreement with that of Dainton [44]. Since the quantum yield (Φ_{OHBA}) of OHBA determined in this study agreed well with the literature Φ•OH, it is reasonable to conclude that BA is useful as a probe for the photochemical generation of •OH from H_2O_2. The Φ•OH value at 365 nm was determined to be about 0.009 (Table 2) much lower than those at shorter wavelengths. The formation rate of •OH at 365 nm in the presence of 10 mM H_2O_2 was approximately 1.54×10^{-7} M using methanol as a probe [11] for a purpose of validation. This supports that H_2O_2 may photo-decompose measurably even at relatively high wavelength up to 365 nm and produce •OH.

4.6. Quantum yields for •OH from Fe(III) species and nitrate

In order to distinguish the Fe(III)-hydroxo complexes, the UV irradiation was carried out under various solution pHs (Table 3 and Supplementary Data, Fig. S3). Fig. 3 shows Φ•OH in the direct photolysis of Fe(III) (pH 6.0) and NO_3^- (pH 5.8) at 254 nm and 10 mM BA. As the concentration of Fe(III) increased up to 1 mM, its Φ•OH linearly increased, and thereafter Φ•OH became a constant value. The Φ•OH values during the photolysis of $Fe(OH)^{2+}$ (pH 3.0) and $Fe(OH)_2^+$ (pH 6.0) at 254 nm were 0.34 and 0.037, respectively, as shown in Table 3. The Φ•OH for $Fe(OH)^{2+}$ is higher than that for $Fe(OH)_2^+$ by a factor of approximately 10. This difference can be mainly attributed to the speciation of various Fe(III)-hydroxo complexes determined by the solution pH. Upon light absorption at 254 nm, Φ•OH shows that the direct production of •OH by aqueous Fe(III) species decreases as pH increases due to the formation of $Fe(OH)_3$ [45]. Since the experimental uncertainty of polymeric Fe(III) species could not be completely excluded [45,46], a higher •OH production can be achieved with photo-excited Fe(III) species at more acidic pH. Upon absorption of UV irradiation, these complexes undergo various photolysis with the generation of •OH.

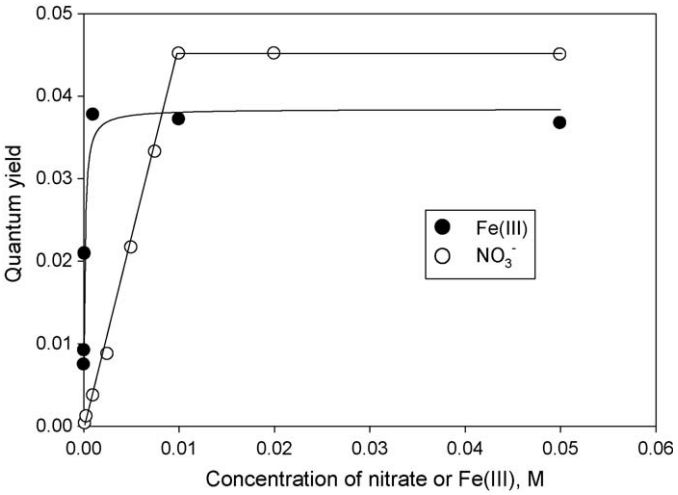

Fig. 3. The hydroxyl radical formation rate as a function of wavelength and levels of benzoic acid. Solid lines show trendlines.

Table 3
Quantum yield (Φ•OH) for the hydroxyl radical in the photolysis of Fe(III)-hydroxo species and nitrate at various wavelengths.

Fe(III)	Wavelength (nm)	Quantum yield (Φ•OH)	References
Fe^{3+}	254	0.0046 ± 0.00052	[8]
	≤300	≈0.05	[7]
$Fe(OH)^{2+}$	254	0.69 ± 0.025	[8]
	254	0.34 ± 0.03[a]	This study
	308	0.2	[46]
	280–370	0.31–0.07	[7]
$Fe(OH)_2^{+}$	254	0.037 ± 0.001[b]	This study
NO_3^-	254	0.045 (pH 6)	This study
	290	0.010 (pH 8)	[48]
	295	0.011(pH 8)	[48]
	300	0.009 (pH 8)	[48]
	305	0.0092	[6]
	313	0.013	[24]
	313	0.017	[26]

[a] $Fe(OH)^{2+}$ is a major Fe(III) species at pH 3.
[b] $Fe(OH)_2^{+}$ is a major ionic Fe(III) species at pH 6.

The main reactions taking place in the aqueous phase are summarized below [7,45–47]:

$$Fe(H_2O)_6^{3+} + h\nu \rightarrow Fe(H_2O)_5^{2+} + H^+ + {}^\bullet OH \quad (13)$$

$$Fe^{3+} + OH^- \leftrightarrow Fe(OH)^{2+} \quad (14)$$

$$Fe(OH)^{2+} + h\nu \rightarrow Fe^{2+} + {}^\bullet OH \quad (15)$$

$$Fe(OH)_2^{+} + h\nu \rightarrow FeOH^{+} + {}^\bullet OH \quad (16)$$

However, Φ•OH (0.69) for $Fe(OH)^{2+}$ measured by Lee and Yoon [8] in a pH range of 1–1.7 at 254 nm was twice of that (0.34) in this study. This may result from differences in experimental conditions (pH and reaction mode), as well as in •OH detection method (DMSO-HPLC vs. BA-fluorescence). Thus, it is necessary to clarify potential biases of experimental conditions and to validate methods for detecting •OH production.

Φ•OH during the direct photolysis of NO_3^- at 254 nm was also measured. Unlike Fe(III) species, Φ•OH increased linearly up to the NO_3^- concentration of approximately 10 mM and approached a constant value of 0.045 as NO_3^- concentration increases (Fig. 3 and Table 3). This value is higher than those reported at other wavelengths (Table 3). Fig. 3 indicates that the overall efficiency of •OH production from nitrate is not significantly different from that from ferric species if the nitrate concentration is sufficiently high. However, nitrate is not as efficient precursor of •OH as Fe(III) species in the lower range of the concentration investigated here. Because the nitrate concentration found in the natural environment is much lower than those in our study, it may be suggested that nitrate is not as efficient as ferric species for the production of •OH in the natural environmental condition.

Chemical reactions leading to the formation of •OH from the photolysis of NO_3^- may be summarized as follows [6]:

$$NO_3^- + H_2O + h\nu \rightarrow NO_2^{\bullet} + OH^- + {}^\bullet OH \quad (17)$$

$${}^\bullet OH \leftrightarrow O^{\bullet -} + H^+, \quad pK_a = 11.8 \quad (18)$$

The •OH formed from NO_3^- photolysis can be further involved in reducing nitrate to the nitrogen dioxide radical [45]. Therefore, Φ•OH in the presence of nitrate ions shows wavelength dependence.

5. Conclusions

This study investigated a simple in situ method to measure •OH formation in UV/H_2O_2, UV/Fe(III), and UV/NO_3^- systems using trapping of •OH by BA, producing OHBA isomers. The distribution of OHBA isomers was in the order of *o*-OHBA > *p*-OHBA > *m*-OHBA, although it changed with the H_2O_2 concentration and light intensity. This supports that •OH attacks dominantly on the benzene rings. The quantum yields for •OH formation in the UV/H_2O_2 process were 1.02 and 0.59 at 254 and 313 nm, which were in good agreement with the literature values, confirming that the method is suitable for the measurement of •OH production from UV/H_2O_2 processes. The Φ•OH values increased with increasing concentrations of H_2O_2, Fe(III), and NO_3^- and approached constant values as the concentration further increased. The Φ•OH values were 0.009 for H_2O_2 at 365 nm, showing that •OH production was not negligible at such high wavelength. The Φ•OH values during the photolysis of $Fe(OH)^{2+}$ (pH 3.0) and $Fe(OH)_2^{+}$ (pH 6.0) at 254 nm were 0.34 and 0.037, respectively. The Φ•OH values for NO_3^- approached a constant value of 0.045 at 254 nm at the initial concentration of 10 mM. This study can contribute significantly to understand the mechanism and effects of •OH precursors in the photochemical processes occurred in the natural and engineered environment.

Acknowledgement

This research was supported by a grant (4-1-2) from Sustainable Water Resources Research Center of 21st Century Frontier Research Program, Korea.

Appendix A. Supplementary data

Supplementary data associated with this article can be found, in the online version, at doi:10.1016/j.jiec.2009.10.007.

References

[1] O. Legrini, E. Oliveros, A.M. Braun, Chem. Rev. 93 (1993) 671.
[2] K.A. Hislop, J.R. Bolton, Environ. Sci. Technol. 33 (1999) 3119.
[3] E.J. Rosenfeldt, K.G. Linden, Environ. Sci. Technol. 41 (2007) 2548.
[4] S.R. Sarathy, M. Mohseni, Environ. Sci. Technol. 41 (2007) 8315.
[5] E.J. Rosenfeldt, K.G. Linden, S. Canonica, U. von Gunten, Water Res. 40 (2006) 3695.
[6] P. Warneck, C. Wurzinger, J. Phys. Chem. 92 (1988) 6278.
[7] H.J. Benkelberg, P. Warneck, J. Phys. Chem. 99 (1995) 5214.
[8] C. Lee, J. Yoon, Chemosphere 57 (2004) 1449.

[9] J.H. Baxendale, J.A. Wilson, Trans. Faraday Soc. 53 (1957) 344.
[10] G.V. Buxton, C.L. Greenstock, W.P. Helman, A.B. Ross, J. Phys. Chem. Ref. Data (1988) 17.
[11] X. Zhou, K. Mopper, Mar. Chem. 30 (1990) 71.
[12] W.A. Armstrong, B.A. Black, D.W. Grant, J. Phys. Chem. 64 (1960) 1415.
[13] G.W. Klein, K. Bhatla, V. Madhavan, R.H. Schuler, J. Phys. Chem. 79 (1975) 1767.
[14] M. Grootveld, B. Halliwell, J. Biochem. 237 (1986) 499.
[15] K.-I. Ishibashi, A. Fujishima, T. Watanabe, K. Hashimoto, J. Photochem. Photobiol. A 134 (2000) 139.
[16] J.J. Gao, K.H. Xu, J.X. Hu, H. Huang, B. Tang, J. Agric. Food Chem. 54 (2006) 7968.
[17] Z. Maskos, J.D. Rush, W.H. Koppenol, Free Radical Biol. Med. 8 (1990) 153.
[18] M.E. Lindsey, M.A. Tarr, Chemosphere 41 (2000) 409.
[19] M.E. Lindsey, M.A. Tarr, Environ. Sci. Technol. 34 (2000) 444.
[20] M.S. Elovitz, U. von Gunten, Ozone: Sci. Eng. 21 (1999) 239.
[21] R.W. Matthews, D.F. Sangster, J. Phys. Chem. 69 (1965) 1938.
[22] (a) B.G. Kwon, J. Photochem. Photobiol. A 199 (2008) 112;
(b) W.C. Oha, Y.M. Lee, W.B. Ko, J. Ind. Eng. Chem. 15 (2009) 190;
(c) H.K. Shona, D.L. Chob, J.H. Kim, J. Ind. Eng. Chem. 15 (2009) 476.
[23] M.A. Oturan, J. Pinson, J. Phys. Chem. 99 (1995) 13948.
[24] R.G. Zepp, J. Hoigne, H. Bader, Environ. Sci. Technol. 21 (1987) 443.
[25] L. Sun, J.R. Bolton, J. Phys. Chem. 100 (1996) 4127.
[26] J. Dzengel, J. Theurich, D. Bahnemann, Environ. Sci. Technol. 33 (1999) 294.
[27] J.P. Hunt, H. Taube, J. Am. Chem. Soc. 74 (1952) 5999.
[28] J.F. Gibson, D.J.E. Ingram, M.C.R. Symons, M.G. Townsend, Trans. Faraday Soc. 53 (1957) 914.
[29] J.G. Calvert, J.N. Pitts Jr., Photochemistry, 2nd ed., John Wiley and Sons, Inc., New York, 1967, p. 780.
[30] USEPA, Determination of Carbonyl Compounds by High Performance Liquid Chromatography (HPLC). Method 8315A (SW-846), Revision 1, Office of Solid Waste, Washington, DC, USA, 1996.
[31] B.G. Kwon, J.H. Lee, Anal. Chem. 76 (2004) 6359.
[32] O.C. Zafiriou, R. Bonneau, Photochem. Photobiol. 45 (1987) 723.
[33] G.D. Clark, J.M. Hungerford, G.D. Christian, Anal. Chem. 61 (1989) 973.
[34] G.B. Martine, H.K. Cho, M.E. Meyerhoff, Anal. Chem. 56 (1984) 2612.
[35] S. Dong, P.K. Dasgupta, Environ. Sci. Technol. 21 (1987) 581.
[36] J.H. Lee, I.N. Tang, J.B. Weinstein-Lioyd, Anal. Chem. 62 (1990) 2381.
[37] C.G. Hatchard, C.A. Parker, Proc. R. Soc. Lond., Ser. A 235 (1956) 518.
[38] APHA, Standard Methods for the Examination of Water and Wastewater, 3500-Fe Iron, 20th ed., American Public Health Association, Washington, DC, USA, 1998
[39] B.H.J. Bielski, D.E. Cabelli, R.L. Arudi, A.B. Ross, J. Phys. Chem. Ref. Data 14 (1985) 1041.
[40] W.H. Glaze, Y. Lay, J.-W. Kang, Ind. Eng. Chem. Res. 34 (1995) 2314.
[41] M. Anbar, D. Meyerstein, P. Neta, J. Phys. Chem. 70 (1966) 2660.
[42] M.K. Eberhardt, M. Yoshida, J. Phys. Chem. 77 (1973) 589.
[43] K.D. Asmus, H. Mockel, A. Henglein, J. Phys. Chem. 77 (1973) 1218.
[44] F.S. Dainton, J. Am. Chem. Soc. 78 (1956) 1278.
[45] D. Vione, V. Maurino, C. Minero, E. Pelizzetti, Environ. Sci. Technol. 36 (2002) 669.
[46] I.P. Pozdnyakov, E.M. Glebov, V.F. Plyusnin, V.P. Grivin, Y.V. Ivanov, D.Y. Vorobyev, N.M. Bazhin, Pure Appl. Chem. 72 (2000) 2187.
[47] J. Kiwi, A. Lopez, V. Nadtochenko, Environ. Sci. Technol. 34 (2000) 2162.
[48] P. Vaughan, N.V. Blough, Environ. Sci. Technol. 32 (1998) 2947.